


## REVIEW ARTICLE

# Mannose-6-phosphate complex and improvement in biomechanical properties of the skin

Marie Meunier MS<sup>1</sup>  | Emilie Chapuis BS<sup>1</sup> | Laura Lapierre BS<sup>1</sup> | Pascale Auriol BS<sup>2</sup> | Chantal Paulus BS<sup>2</sup> | Boris Elbaum BS<sup>2</sup> | Eglantine Don Simoni MS<sup>2</sup> | Jérôme Sandré MD<sup>3</sup> | Daniel Auriol PhD<sup>2</sup> | Amandine Scandolera PhD<sup>1</sup> | Romain Reynaud MS<sup>2</sup>

<sup>1</sup>Givaudan Active Beauty, Research and Development, Pomacle, France

<sup>2</sup>Givaudan Active Beauty, Research and Development, Toulouse, France

<sup>3</sup>Polyclinique Courlancy, Reims, France

## Correspondence

Marie Meunier, Skin biology scientist, Givaudan Active Beauty, Route de Bazancourt, 51110 Pomacle.  
Email: marie.meunier@givaudan.com

## Abstract

**Background:** The dermis is composed of a tangle of macromolecules that provides the skin its biomechanical properties. During chronological aging, fibroblasts lose their ability to synthesize collagen and an accumulation of matrix metalloproteinases leads to an increase in collagen degradation. As a result, there is a decline in the biomechanical properties of the skin. Skin aging is accelerated by external factors such as UV radiation and pollution, which induce accumulation of oxidants, and so of oxidized proteins in the skin.

**Aims:** Atomic force microscopy (AFM) has emerged as an alternative method for studying the biomechanical properties of skin cells and tissues.

**Methods/Results:** Thus, we identified mannose-6-phosphate complex as a new powerful molecule capable of reversing the visible signs of aging by reorganizing the collagen network of the dermis and by improving the skin biomechanical properties. This effect was correlated with clinical studies that showed a marked antiaging effect through a reduction in the number of crow's feet and in the depth and size of neck wrinkles.

**Conclusion:** Mannose-6-phosphate complex appeared to be able to protect proteins in the dermis scaffold against oxidation and degradation, allowing an improvement in the skin biomechanical properties.

## KEYWORDS

anti-aging, atomic force microscopy, mannose-6-phosphate complex, Skin biomechanical properties

## 1 | INTRODUCTION

The skin is composed of three layers including the epidermis, dermis, and hypodermis, each of which play a specific role in the skin.<sup>1</sup> Interestingly, the dermis provides all the biomechanical properties of the skin such as elasticity and firmness, and imparts resilience through its specific composition and organization. It is a highly vascularized tissue, mainly composed of fibroblasts capable of synthesizing structural proteins such as collagens,<sup>2</sup> which are the most

abundant. The two main types of collagen synthesized in the dermis are type I and type III collagen,<sup>3</sup> both of which are composed of three polypeptide chains organized in a triple helix which is involved in mechanic resistance of tissues against traction.<sup>4</sup> In the upper dermis, also known as the papillary dermis, collagen fibers are arranged perpendicularly to the epidermis, intertwined with thinner vertical elastic fibers named oxytalan and elaunin fibers having few elastic properties due to a low amount of elastin.<sup>5</sup> In contrast, collagen fibers from the underlying reticular dermis are larger and arranged

This is an open access article under the terms of the Creative Commons Attribution-NonCommercial-NoDerivs License, which permits use and distribution in any medium, provided the original work is properly cited, the use is non-commercial and no modifications or adaptations are made.

© 2021 The Authors. *Journal of Cosmetic Dermatology* published by Wiley Periodicals LLC.

parallel to the epidermis, associated with thicker horizontal elastic fibers and having a strong elastic property.<sup>6</sup> These fibers are associated with other structural proteins, such as type V collagen, which promotes collagen fibers through its association with type I collagen for example, but also with hyaluronate and many other molecules, forming the extracellular matrix.<sup>2,7</sup> Elastic and collagen fibers are both present in the skin since they have different functions. Indeed, elastin fibers provide the skin its ability to undergo repetitive extension or deformation and return to its original size, while collagen fibers play a structural role in providing tensile strength and firmness to the skin.<sup>8</sup> This tangle of macromolecules constitutes a scaffold that confers biomechanical properties of the skin, the stability of which partly depends on its firm attachment to the epidermis.<sup>9</sup> This cohesion between the dermis and epidermis is established by means of a number of proteins such as fibullin-1, tenascin C, and many others, which contribute to the strength of the dermo-epidermal junction.<sup>10-12</sup>

It has been described that during intrinsic aging, there is disequilibrium between synthesis and degradation in favor of degradation of proteins owing to slow turnover related to their long half-life.<sup>13</sup> Indeed, aging fibroblasts express more PGE synthase 1 (PTGES1) and cyclooxygenase 2 (COX2), resulting in synthesis of prostaglandin E<sub>2</sub> (PGE2), which is an inhibitor of collagen production by fibroblasts.<sup>14</sup> Thus, fibroblasts progressively lose their ability to synthesize collagen<sup>15</sup> leading to thinning of the dermis.<sup>9</sup> This phenomenon is accentuated by an accumulation of matrix metalloproteinases in the aging dermis which leads to the increase in collagen degradation with age.<sup>16</sup> Hence, aging induces a decrease in skin elasticity and suppleness,<sup>17</sup> in addition to matrix disorganization.<sup>18</sup> As a consequence of all these effects, there is a sharp decrease in the biomechanical properties of the skin related to aging.<sup>19</sup> This disturbance of the biomechanical properties and of collagen fibers network in the skin is well described in the literature for people over 50 years old.<sup>19-22</sup>

Dermocosmetic research focuses attention on the negative impact of aging on these biomechanical properties and how it can be avoided. Until recently, the biomechanical properties of the skin were mainly studied by in vivo clinical studies using techniques such as cutometry to measure skin tonicity and skin suppleness, ballistometry to assess skin elasticity and firmness or Siascope® to visualize collagen density and organization, among many other methods. There was a gap between clinical studies and the in vitro/ex vivo level in studying the biomechanical properties of the skin. Atomic Force Microscopy (AFM) emerged as few years ago as a method that could offer an alternative for studying the biomechanical properties of skin cells and tissues.

Atomic Force Microscopy was invented in 1982 by Gerd Binnig, an IBM scientist who demonstrated this tool's ability to provide a resolution of fractions of a nanometer.<sup>23</sup> This technique allows scanning the surface of cells or skin slices by means of a sharp tip placed in close proximity to the sample surface. Forces between the tip and the sample, such as mechanical contact force, Van der Waals forces, electrostatic forces, or many other types, lead to a deflection of the cantilever which is the tip support.<sup>24</sup> In tapping mode, the cantilever oscillates up and down with an amplitude ranging between several nanometers and 200 nanometers, which cause the tip

to indent in the substrate and follow the relief of the support; this is the Peak Force QNM method.<sup>25</sup> This method not only provides a three-dimensional surface profile; it also yields information concerning sample stiffness and suppleness by means of indentation.<sup>26</sup>

Atomic Force Microscopy is a very convenient technique, since the samples to be analyzed do not require any special preparation such as carbon coating, which is required for electronic microscopy. The AFM method can be coupled with several optical microscopy and spectroscopy techniques, such as fluorescent microscopy or infrared spectroscopy. For example, in conjunction with Small Angle X-ray Scattering (SAXS) analysis, we can relatively quantify the collagen network organization by measuring X-ray diffraction through the sample, providing complementary information to AFM imaging.<sup>27</sup> Indeed, well organized and cohesive fibers yield intense and sharp peaks, whereas a disturbed network yields less intense and wide peaks. The measurement of peak area provides a quantitative value for organization of the collagen fiber network. AFM gives information such as force curves as well as data concerning stiffening, suppleness, and surface topography.

Mannose and mannose-6-phosphate are well known to be a source of energy for cellular metabolism through their involvement in glycolysis. Indeed, during this process there is a production of adenosine-tri-phosphate (ATP), which provides a source of energy for cells and so, this can boost the cellular metabolism.<sup>28,29</sup> This is why this complex has been identified as a potential candidate that could improve the biomechanical properties of the skin. A smart mix of mannose and mannose-6-phosphate, simply called mannose-6-phosphate complex, has been crafted by white biotechnology in our laboratories. We studied its biological activity through various in vitro and ex vivo models in order to understand the biological pathways through which mannose-6-phosphate complex would be able to provide an anti-aging benefit to the skin. We carried out further research with AFM coupled to SAXS analysis to evaluate its impact on skin restructuring ex vivo. Finally, we confirmed its efficacy on the biomechanical properties of the skin by clinical studies.

## 2 | METHOD

### 2.1 | Raw material

D-Mannose-6-Phosphate was obtained by the reaction between condensed phosphoric acid, in particular pyrophosphate, and mannose in the presence of acid phosphatase from *Shigella flexneri*. D-Mannose-6-Phosphate was subsequently purified first by removing the excess condensed phosphoric acid and the released phosphate and optionally by removing the residual mannose.

#### 2.1.1 | Acid phosphatase from *Shigella flexneri*

The gene from the acid phosphatase from *Shigella flexneri* (usual name PhoN-Sf) was synthesized by DNA 2.0, now ATUM (Newark,

CA, USA) (UniProt accession number O50542). The gene was cloned into plasmid pET-26b(+) (Merck Millipore, Darmstadt, Germany), and the expression vector was subsequently transformed into *E coli* BL21 (DE3) cells (Thermo Fisher Scientific, Waltham, MA, USA).

### 2.1.2 | Mannose-6-Phosphate synthesis

The enzymatic reaction was carried out as follows:

- D-Mannose, 0.15 M,
- disodium pyrophosphate, pH 4.15:0.33 M,
- PhoN-Sf enzyme: 0.20 U/mL
- Magnesium and zinc chloride salts: 0.50 and 0.1 mM, respectively
- Temperature: 30°C; moderate agitation
- Duration: 22 hours.

### 2.1.3 | Mannose-6-phosphate purification and quantification

Residual disodium pyrophosphate and released phosphate were removed by sequential addition of magnesium and ammonium salts to achieve a pH close to 9.5. The precipitate formed, containing pyrophosphate, phosphate, magnesium and ammonium, was removed by filtration. Magnesium and ammonium were removed using a cation exchange resin, and the pH of the solution was finally adjusted using concentrated sodium hydroxide to obtain D-Mannose-6-phosphate, sodium salt at a pH value ranging from 4.0 to 7.0.

The D-Mannose-6-Phosphate and D-Mannose content was measured using the K-MANGL enzymatic kit from Libios (Pontcharra sur Turdine, France). The complete kit indicated the amount of D-Mannose-6-Phosphate and D-Mannose, whereas a modified kit in which ATP was removed allowed measurement of the concentration of D-Mannose-6-phosphate only; the difference between the two values gave the D-Mannose concentration.

### 2.1.4 | Composition of the mannose-6-phosphate complex

The mannose-6-phosphate complex was an aqueous solution with the following composition per gram:

- 0.11097 mmoles of D-Mannose-6-Phosphate (31.307 mg; molecular mass: 282.12)
- 0.07030 mmoles of D-Mannose 12.663 mg; molecular mass: 180.16).

The final composition of the mannose-6-phosphate complex is described below:

- 2.0 to 4.0% mannose-6-phosphate sodium salt
- 0.8 to 3.0% mannose
- Up to 0.2% sodium phosphate
- 50% glycerol
- Qsp 100% water

### 2.2 | Evaluation of cellular mass in presence of mannose-6-phosphate complex

Normal human dermal fibroblasts (NDHFs) were seeded at 100,000 cells per well in 6-wells plate. After 48 hours of culture, cells were stimulated with mannose-6-phosphate complex diluted at 4% (v/v) in free DMEM medium (Gibco®, Life Technologies, CA, USA) supplemented with 1% antibiotics (Sigma-Aldrich, MI, USA). After 48 hours of treatment, cells were fixed with methanol (Merck Millipore, Darmstadt, Germany) and stained with Crystal Violet solution (Sigma-Aldrich, MI, USA). Excess of dye was eliminated by successive distilled water bathes, and plates were allowed to dry. Stained cells were dissolved with acetic acid (Sigma-Aldrich, MI, USA) at 10%, and optical density was measured at 560 nm.

### 2.3 | Transcriptomic analysis on normal human fibroblasts

Normal human dermal fibroblasts (NHDFs), freshly isolated from a 46 years old donor undergoing abdominal surgery, were seeded at 300 000 cells per well in 6-wells plates. After 48 hours of culture, the cells were stimulated with mannose-6-phosphate complex at 4% in free DMEM medium (Gibco®, Life Technologies) supplemented with 1% antibiotics (Sigma-Aldrich). After 6 hours of treatment, RNAs were extracted according to the Trizol method (Thermo Fisher Scientific). RNA quality was controlled, and a reverse transcription was performed to obtain cDNA using the Verso cDNA kit (Thermo Fisher Scientific). RT-qPCR was performed on specific pre-coated plates (Applied Biosystems) designed to study transcriptomic expression of different genes involved in dermal function with 10 ng of cDNA per well using CFX96 Touch (BioRad) and Universal Taqman mix (Quantabio). The relative quantification (RQ) of gene expression was calculated according to POLR2A (RNA polymerase II, subunit A) and PES1 (Pescadillo Ribosomal Biogenesis Factor 1) housekeeping genes.

### 2.4 | Protein expression and skin matrix restructuring

#### 2.4.1 | Skin explant preparation and culture

NativeSkin® (Genoskin, Toulouse, France) from a 59-year-old Caucasian donor was maintained in culture with the epidermal surface in contact with air to allow topical application.

Mannose-6-phosphate complex at 4% was placed in contact with the NativeSkin<sup>®</sup> by topical application and renewed every day for 7 days. Untreated Nativeskin<sup>®</sup> was used as negative control. NativeSkin<sup>®</sup> was used in triplicate. After 7 days of treatment, NativeSkin<sup>®</sup> was fixed in formalin for histologic studies.

## 2.4.2 | Immunohistochemistry

Markers of interest were detected by immunofluorescence. Briefly, skin explants were fixed in formalin and embedded in paraffin and sectioned. Slides were twice de-paraffinized using xylene solution. Then, tissues were dehydrated by passing through descending concentrations of alcohol and washed off with distilled water. Antigen unmasking was performed in sodium citrate buffer. The sections were incubated with the primary antibodies anti-Collagen V (PA538880, Thermo Fisher), anti-Fibulin 1 (NBP1-84725, Novus Biologicals, Centennial, USA), and anti-Tenascin C (ab108930, Abcam, Cambridge, United Kingdom) according to the manufacturer's instructions. The biomarkers expressions were analyzed by fluorescence microscopy (DM5000B - Leica Microsystems, Wetzlar, Germany), and 10 images were acquired by biomarker. The fluorescence was quantified for each picture by ImageJ software. The region of interest was delimited, and the total fluorescence intensity was calculated then reported to the total area of interest.

## 2.4.3 | Morphological analysis by Masson's Trichrome staining

5 $\mu$ m sections were cut and stained using a Masson's Trichrome kit (RAL Diagnostics, Martillac, France) according to the manufacturer's instructions. Staining analysis was performed with LEICA<sup>®</sup> DFC 280 (Leica Microsystems, Wetzlar, Germany) and several images representative of the slices were acquired. Immunostaining images were qualitatively analyzed to describe the state of different skin compartments; the most representative are indicated and described. Hematoxylin stains the nucleus purple and fuchsine ponceau stains muscular fibers, erythrocytes, cytoplasm, and elastic fibers pink. The last used dye was Vert Lumière which specifically stained collagen fibers.

## 2.5 | Study of biomechanical properties of the skin

### 2.5.1 | Skin explant preparation

Human skin explants with an average diameter of 12 mm ( $\pm$ 1 mm) were prepared on each abdominoplasty originating from two different donors: A young 30-year-old Caucasian woman and a mature 65-year-old Caucasian woman under informed consent. The explants were kept alive in BEM culture medium (BIO-EC) at 37°C in a humid, 5%-CO<sub>2</sub> atmosphere.

Mannose-6-phosphate complex at 4% was topically applied to skin explants from the mature donor with 2  $\mu$ l per explant (2 mg/cm<sup>2</sup>) and spread using a small spatula. The products were applied on D0, D1, D2, D3, D5, D6, and D7. The control explants did not receive any treatment except for renewal of the culture medium. The culture medium was half renewed every other day with 1 mL. Samples were cryofixed after treatment, and cold-cut cryosections 20  $\mu$ m thick were deposited on glass slides before being stored at -80°C.

### 2.5.2 | Atomic force microscopy measurement of Young's modulus in reticular dermis

The PeakForce<sup>®</sup> QNM (Quantitative Nanomechanical Mapping) and the Force-Volume mode were used for this study. Before each experiment, the deflection sensitivity of the cantilever was calibrated on Sapphire, and its spring constant was also calibrated. Acquisition of a force volume on reticular dermis was performed in aqueous condition. The parameters used were as follows: Force/volume: 30 $\mu$ m x 30 $\mu$ m - 128px<sup>2</sup> / Force indentation curves: Force = 50 nN - Ramp size = 10  $\mu$ m. The selected AFM cantilever had a theoretical spring constant of 3N/m, and the pyramidal tip had a curvature radius of <10 nm, enabling high-resolution imaging. The AFM tip is placed on an area of interest on reticular dermis. Images at different scales are acquired on each zone (15 $\mu$ m and 3 $\mu$ m). The quantifications of the Young's modulus based on raw force curves were obtained with BioMeca Analysis processing software (BioMeca, Lyons, France). Raw force curves obtained for each skin section were treated to quantify global Ea from dermis. Sneddon's theoretical model was applied to the whole curve.

### 2.5.3 | Atomic force microscopy acquisition of skin slice topography

The sections were restored to room temperature for 24 hours before analysis and observed with a Bruker Multimode 8 microscope equipped with a Nanoscope V (Bruker) controller in tapping mode with a tip having a curvature radius of approximately 10 nm (equivalent to the resolution of the assembly). The 512 x 512 pixel images were acquired at a scan rate of 1 Hz. Three series of 3 x 3  $\mu$ m<sup>2</sup> images were acquired at different points 100  $\mu$ m and more apart, rather in the deep dermis. The condition for the zones to be observed was that they were relatively flat, without any significant asperities that might damage the tip or the lever of the AFM. The images were subsequently processed with Gwyddion software (GNU General Public License).

### 2.5.4 | Small angle X-ray diffraction measurement

The cryofixed samples were restored to room temperature for 8 hours before the observations. SAXS data collection: Beamline ID02 (ESRF, France) / X-ray beam energy: 12.46 keV / Mode 7/8

multibunch / Beamsize on the sample: 150 (h) x 100 (v)  $\mu\text{m}^2$  / Distance sample detector: 4m / 2D detector / Time exposure per pattern: 1 second / T = 22°C, RH 40%.

At least 20 diffraction patterns were collected per sample at various positions. The data were processed using SAXSutilities software (ESRF, Grenoble, France). The diffraction profiles were obtained by 360° angular integration of the 2D diffraction signal and subtraction of the average diffraction signal from the mica support.

## 2.6 | INCI formula used in the clinical study

AQUA/WATER, CETYL ALCOHOL, GLYCERYL STEARATE, PEG-75 STEARATE, CETETH-20, STEARETH- 20, ISODECYL NEOPENTANOATE,  $\pm$  MANNOSE-6-PHOSPHATE COMPLEX, PHENOXYETHANOL, METHYL PARABEN, PROPYL PARABEN, ETHYL PARABEN, DIMETHICONE, FRAGRANCE, BENZYL SALLICYLATE, LINALOOL, D-LIMONENE.

## 2.7 | Anti-aging study on the face area

### 2.7.1 | Panel description

A double-blind, placebo-controlled clinical study was carried out on 22 volunteers (of between 50 and 70 years of age, mean age:  $59 \pm 4.9$  years) fulfilling the inclusion and exclusion criteria defined in the study protocol. All the subjects participating in the study gave their informed consent signed at the beginning of the study. The study followed and was in compliance with the tenets of the Declaration of Helsinki. The volunteers were required to have wrinkles or crow's feet and aging spots on their faces. The volunteers applied the cream containing 4% of mannose-6-phosphate complex and placebo twice daily to each half of the face for 28 (D28) and 56 (D56) days. Collagen density was analyzed using SIAscope® (MedX Health Corp) and aging signs such as wrinkles by a VISIA analysis (Canfield Scientific).

### 2.7.2 | Collagen analysis by SIAscope®

SIAscope® is a method of spectrophotometric intracutaneous analysis that allows an understanding of how light interacts with the skin structure and thus makes it possible to visualize the distribution of chromophores in the skin: melanin, hemoglobin, and collagen up to 2 mm under the skin.

A SIAscope® portable scanning device connected to Siametrics® software was placed in contact with the skin and the SIAscope® illuminated the skin. Some of the light is reflected and scattered away from the surface. The remainder is transmitted into the top layers of the skin. Varying fractions of the incoming light are absorbed by the melanin in the epidermis before penetrating the dermis where they are absorbed by the hemoglobin in the blood vessels. Scattering also occurs in the dermis when the light interacts with the collagen, resulting in a portion of the light being remitted back to the surface.

By interpreting the combination of wavelengths returned to the SIAscope®, Siametrics® is subsequently able to produce SIAscans®; these are generated by referring to inbuilt proprietary mathematical models of skin optics. In this study, the density of collagen and its distribution were analyzed at the commissure level on the face.

### 2.7.3 | Crow's feet wrinkle analysis by VISIA CR 2.3®

Using VISIA CR 2.3® from Canfield® imaging systems, digital photographs of the face were taken at D28 and D56 with repositioning at D0. Repositioning is controlled directly on a data-processing screen using an overlay visualization of the images at each acquisition time. The VISIA allows pictures to be taken with different types of illumination and very rapid image capture. A series of photographs taken under multi-spectral imaging and analysis allows capture of visual information affecting the appearance of the skin. Crow's feet wrinkles were analyzed using this method.

## 2.8 | Anti-aging study on the neck area

### 2.8.1 | Panel description

A double-blind, placebo-controlled clinical study was conducted on 39 volunteers (of between 45 and 75 years of age, mean age:  $56 \pm 6.2$  years) fulfilling the inclusion and exclusion criteria defined in the study protocol. Volunteers were required to have wrinkles in the neck area. The volunteers applied the cream containing 4% of mannose-6-phosphate complex and placebo twice daily to the entire face and neck for 28 (D28) and 56 (D56) days. Neck wrinkles were analyzed based on the size and number of wrinkles using AEVA-HE® (Techmasys, Limours, France) analysis.

### 2.8.2 | Neck wrinkle analysis by AEVA-HE®

The AEVA-HE® system measures the effectiveness of a cosmetic product without skin contact. For this study, we used the AEVA-HE® system with the 250 sensors in order to measure the depth, length and number of wrinkles. The AEVA-HE® system offers high resolution 3D scanning based on a fringe projection unit using light associated with stereometry. The volunteers were installed in the VisioTOP-500 benches for accurate and steady positioning and repositioning between the different measuring times.

## 2.9 | Statistical analysis

All results were expressed as the mean  $\pm$  SEM. Data were statistically analyzed by Prism 7.0 (GraphPad Software). A Student's t test was performed for all studies, except for measurement of Young's modulus in reticular dermis for which a Wilcoxon test was performed.

### 3 | RESULTS

#### 3.1 | Determination of the testing dose of mannose-6-phosphate complex

To assess the biological evaluation of mannose-6-phosphate complex, the active was first tested on normal human fibroblast in a range of dilution from 0.125% to 8% (v/v) in order to identify the optimal dose to be used and the cytotoxic evaluation after 48 hours of treatment evidenced that there were not specific cytotoxic effect with all tested doses (data not shown). We selected 4% (v/v) dose as the highest non-toxic dose that could be applied on human skin. A complementary assay based on the estimation of cellular mass using CVS was then performed to verify if the selected dose had no impact. We evidenced that mannose-6-phosphate complex at 4% (v/v) did not had any effect on fibroblasts' cellular mass (Figure 1).

#### 3.2 | Impact of mannose-6-phosphate complex on dermis restructuring

During aging, organization of the dermis is markedly altered, especially through a loss of collagen fiber cohesion. Firstly, we were interested in ascertaining whether mannose-6-phosphate complex could reactivate key transcription factors involved in the control of matrix remodeling. Using normal human fibroblasts, we showed that mannose-6-phosphate complex induced significant mRNA upregulation of CTGF, CYR61, and TGFB1 genes with +80%, +84%, and +18%, respectively, versus the untreated condition (Figure 2). All in all, these results strongly suggested that mannose-6-phosphate complex could stimulate matrix remodeling and fibroblast proliferation.

Based on transcriptomic results, we performed an ex vivo study to confirm that the growth factor upregulation leads to dermal restructuring. 4% mannose-6-phosphate complex was topically applied for 7 days to human skin explants and a protein expression analysis was carried out by specific immunohistochemistry targeting Collagen V, Fibulin 1, and Tenascin C, which are three structural proteins for skin. Quantification of Collagen V and Fibulin 1 in the dermal layer showed a significant increase in their expression by +17% and +13%, respectively, with 4% mannose-6-phosphate complex versus the untreated condition (Figure 3). Similarly, quantification of Tenascin C in the epidermal layer demonstrated a significant increase in its expression with 4% mannose-6-phosphate complex by + 51% in relation to the untreated condition (Figure 3). These initial results suggest that mannose-6-phosphate complex was able to significantly improve organization of the skin and especially structure of the dermis.

We performed Masson's Trichrome staining in order to analyses the impact of 4% mannose-6-phosphate complex on skin morphology after 7 days of topical application. We evidenced that the skin explants treated with 4% mannose-6-phosphate complex showed a similar epidermal morphology versus the untreated control.

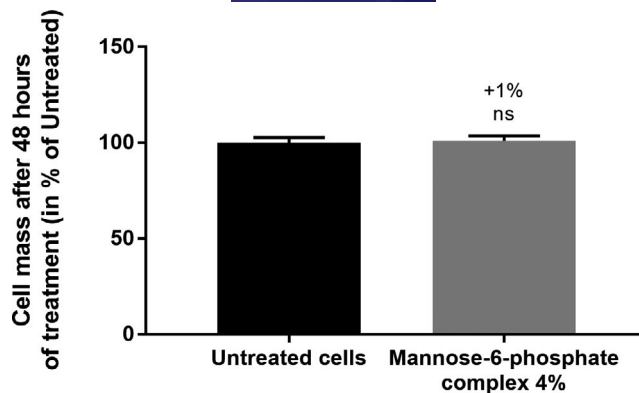


**FIGURE 1** Evaluation of the impact of the 4% (v/v) selected dose on cell mass after 48 hours of treatment. The variation with the treatment was compared with the untreated condition using Mann-Whitney test

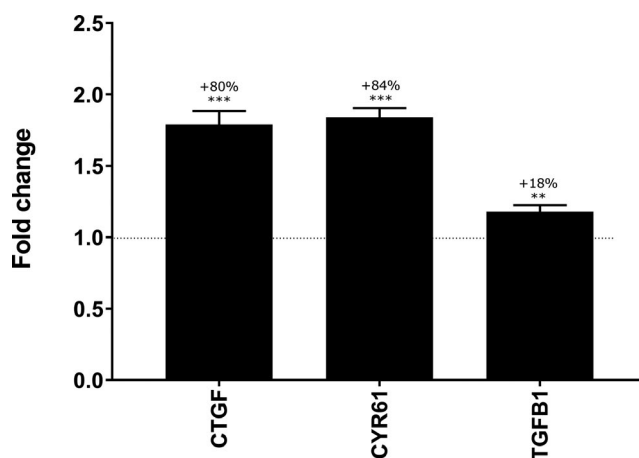


**FIGURE 2** Transcriptomic analysis of mannose-6-phosphate complex effect at 4% on normal dermal fibroblasts after 6 h of treatment. Gene modulation was analyzed by RT-qPCR with Taqman method. The fold change was compared with untreated condition using Student's *t* test with \*\**P* < .01, \*\*\**P* < .001

Regarding the dermis, the papillary dermis showed an identical morphology to the control sample, whereas the reticular dermis evidenced an increased density with 4% mannose-6-phosphate complex versus the untreated condition (Figure 4). This observation confirmed that mannose-6-phosphate complex could influence the structure of the skin and more specifically organization of the dermis.

#### 3.3 | Impact of mannose-6-phosphate complex on the biomechanical properties of the skin ex vivo

The structure of the dermis is directly related to the biomechanical properties of skin due to its specific composition which is significantly altered with aging. We first compared the impact of aging on the organization of the collagen fiber network in the reticular



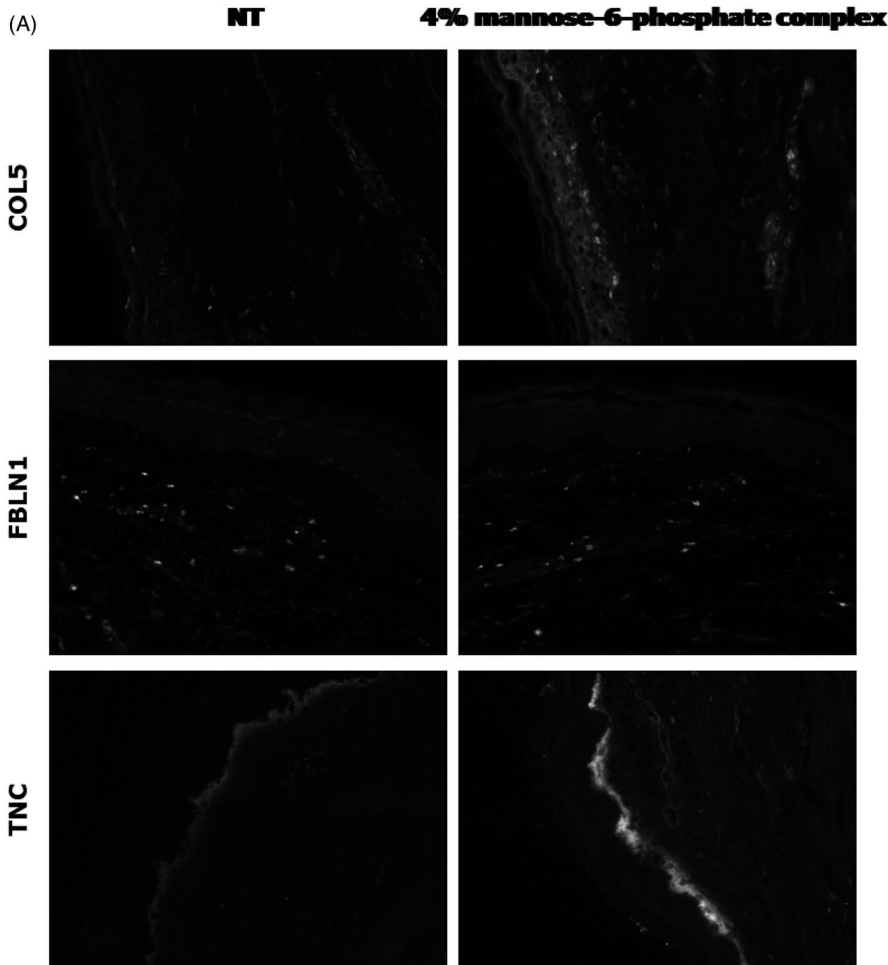
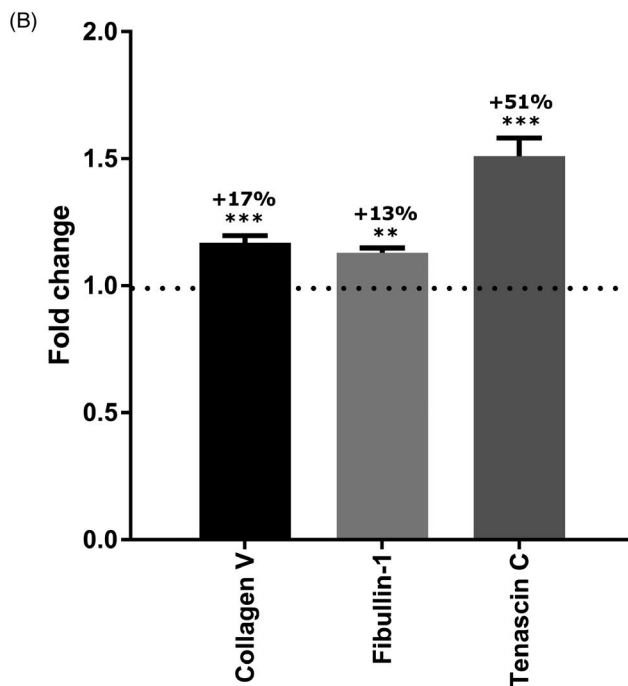


**FIGURE 3** Quantification by immunohistochemistry of Collagen V, Fibullin-1 and Tenascin C protein expression in human skin explant topically treated for 7 d with mannose-6-phosphate complex at 4%. Fold change is the comparison to the untreated condition, using Student's *t* test with  $**P < .01$ ,  $***P < .001$



dermis using the topographic mode of Atomic Force Microscopy (AFM). The AFM Peak Force QNM method evidenced a disorganized collagen network in mature skin, whereas collagen fibers

were parallel and more cohesive in young skin (Figure 5). This disorganization was quantified by the Small Angle X-ray Scattering (SAXS) method which evidenced less intense and wider peaks for

**FIGURE 4** Evaluation of mannose-6-phosphate impact on dermis collagen density after 7 days of topical treatment at 4%. Dermis collagen density was visualized by Masson's trichrome staining

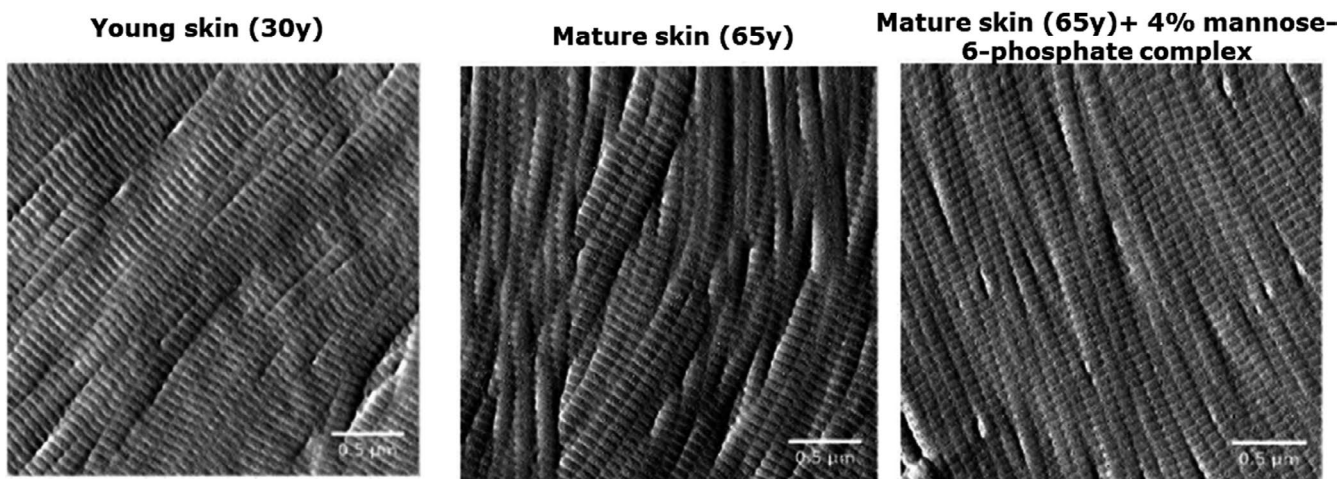
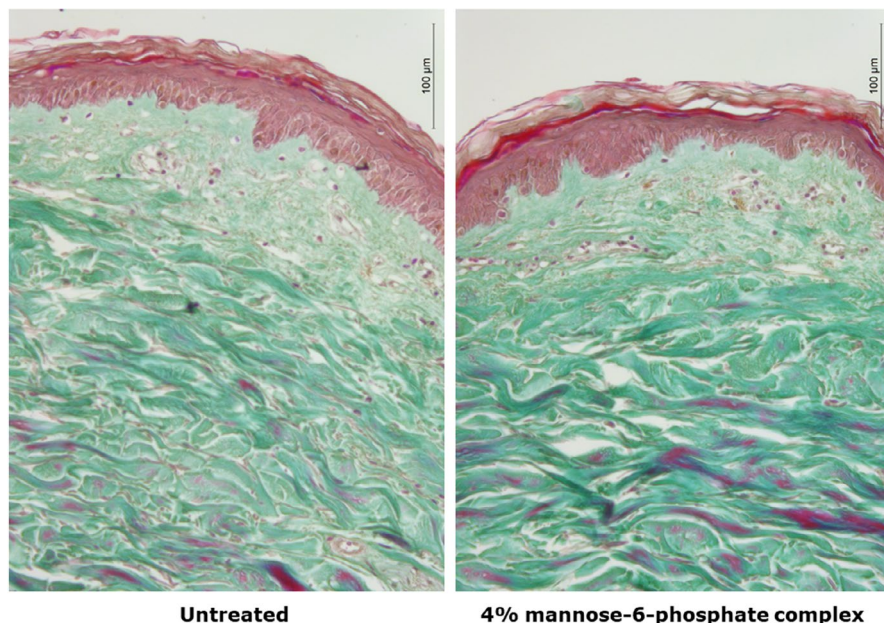


**FIGURE 5** Topographic images of collagen fibers organization on skin explants cryoslices after 7 days of topical treatment at 4%, acquired by Atomic Force Microscopy with tapping mode

mature skin than for young skin, showing that the collagen fiber network from young skin is 2.3 times better organized than in mature skin (Figure 6). We subsequently compared Young's modulus of skin, also known as elastic modulus, in the reticular dermis and noted that aging had a significant impact on skin firmness. Indeed, we observed a significant  $-48\%$  decrease in Young's modulus of skin in mature skin compared with young skin (Figure 7), indicating a loss of skin firmness.

During a second stage, we raised the hypothesis that mannose-6-phosphate complex could improve these biomechanical properties. Here, we evidenced that topical application of 4% mannose-6-phosphate complex had a marked effect on enhancing the mechanical properties of a mature skin as observed by the re-organized collagen fiber network in Figure 4. Quantification of this

organization using the SAXS method confirmed that mannose-6-phosphate complex at 4% induced a 4.8 times better organized collagen fiber network than untreated mature skin, and this organization was even better than that observed in young skin (Figure 6). This effect was also correlated to a significant increase in Young's modulus in reticular dermis by  $+22\%$  with treatment, indicating enhancement of skin firmness (Figure 7). By using the AFM and SAXS method, we observed that according to the age of the donor, there is a negative impact on the dermis organization and firmness and that mannose-6-phosphate complex seems to be able to improve this organization as in the younger donor. These interesting results obtained have to be confirmed on a larger cohort through a clinical study in order to confirm in a real condition that the hypothetical improvement of collagen network organization leads to an anti-aging benefit.



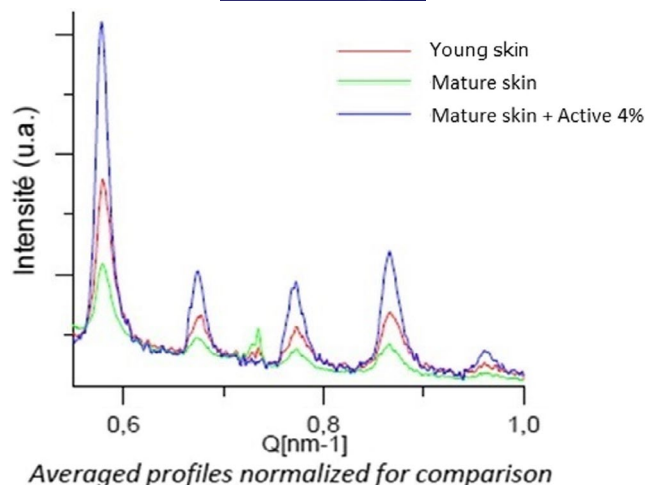


**FIGURE 6** Quantification of collagen fibers cohesion in skin explants cryoslices by Small Angle X-ray Scattering method after 7 d of topical treatment with mannose-6-phosphate complex at 4%. The peaks area is representative of collagen fibers network organization

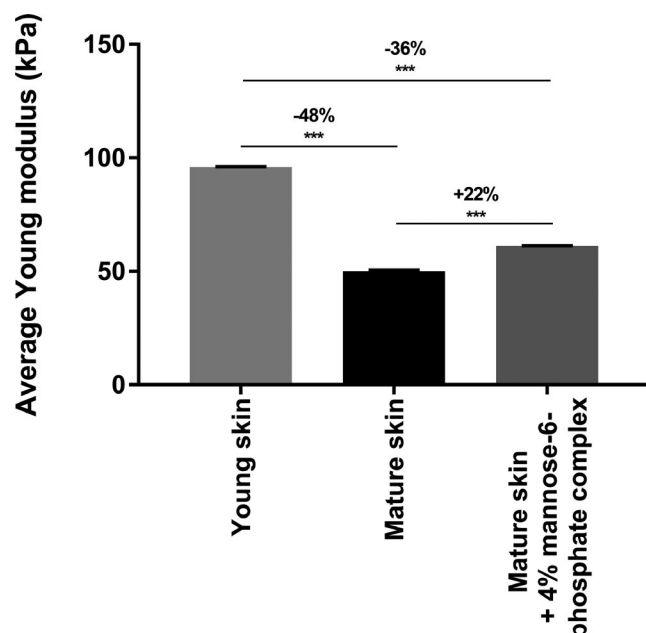


**FIGURE 7** Quantification of reticular dermis' Young modulus in skin explants cryoslices by Atomic Force Microscopy with PeakForce<sup>®</sup> QNM and Force-Volume modes after 7 d of topical treatment with mannose-6-phosphate complex at 4%. Comparison between the different conditions was made using Wilcoxon test with \*\*\* $P < .001$

## 3.4 | Impact of mannose-6-phosphate complex on the biomechanical properties of the skin in vivo

### 3.4.1 | Collagen density

On a clinical level, we sought to confirm the efficacy of mannose-6-phosphate complex on skin firmness via collagen network

reorganization. The collagen density and distribution were measured using SIAscope<sup>®</sup> after 28 and 56 days of twice daily application to half the face of a cream containing 4% mannose-6-phosphate complex versus placebo. The SIAscope<sup>®</sup> method allowed analysis of the collagen network indicating a level of density and organization that are directly proportional to signal intensity. After 28 days (D28), we observed a significant +3.88% improvement in collagen density and organization versus D0. This increase in collagen organization was 3.8 times significantly higher than that observed with placebo (Figure 8). After 56 days (D56), similar results were obtained with a significant +3.66% improvement in collagen density and organization versus D0. We demonstrated that this increase was 2.2 times significantly higher than that observed with placebo (Figure 8). These results confirmed that mannose-6-phosphate complex at 4% was able to significantly improve collagen fiber organization.

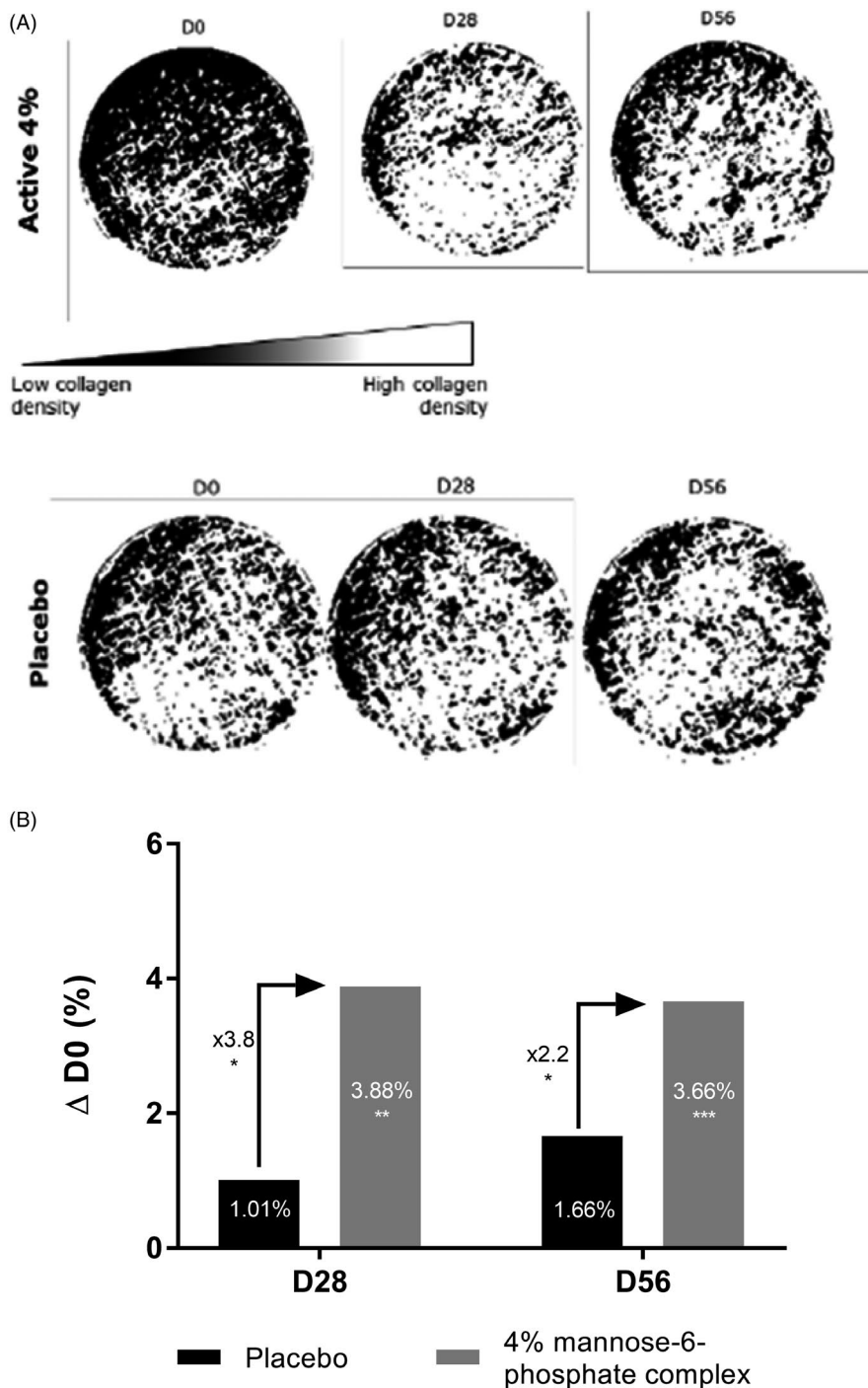
### 3.4.2 | Crow's feet wrinkles

Moreover, we hypothesized that improving the biomechanical properties of the skin could contribute an anti-aging effect by reducing wrinkles. We therefore performed wrinkle analysis focusing on wrinkles in the crow's feet area from 22 volunteers using the VISIA CR 2.3<sup>®</sup> system. We observed that 4% mannose-6-phosphate complex brought a slight -1.6% improvement in the number of wrinkles after D28 versus placebo. After 56 days of application, this effect was increased as shown by the significant reduction in the number of wrinkles in comparison to placebo at D56. Indeed, placebo cream did not show any improving effect with a +9.7% number of crow's feet wrinkles, whereas mannose-6-phosphate significantly reduced this number of wrinkles by -11.6% versus placebo (Figure 9).

### 3.4.3 | Neck wrinkles

We focused our attention on another area that is subject to high mechanical stresses that promote deeper wrinkles, that is, the neck. After 56 days of twice daily application of cream containing 4% of mannose-6-phosphate complex or placebo, we used the AEVA-HE<sup>®</sup> system with the 250 sensors in 39 volunteers to study the depth and size of neck wrinkles. Our results showed that after 28 days, mannose-6-phosphate complex was highly effective in significantly reducing neck wrinkle size by -32.5% vs placebo and the effect was maintained after 56 days by -23.2% versus placebo (Figure 10). Mannose-6-phosphate complex was also significantly effective against neck wrinkle depth as observed by the -8.2% and -8.3% reduction in depth versus placebo after 28 days and 56 days respectively (Figure 11A). These impacts on neck wrinkle size and depth bring a smoothing effect which is clearly visible in the 3D reconstruction (Figure 11B). Overall, these results confirmed that the marked improvement in the collagen fiber network

**FIGURE 8** Binary representation of collagen density and organization in the skin obtained by SIAscope measurement (A) and quantification compared with D0 (B) after 28 and 56 d of twice daily application in hemiface of a cream containing 4% mannose-6-phosphate complex versus placebo. Comparisons were made using Student's *t* test with \**P* < .05, \*\**P* < .01, \*\*\**P* < .001



has effective anti-aging properties by reducing wrinkles in various areas.

#### 4 | DISCUSSION

In the first part of this study, we were interested in studying the impact of intrinsic aging on the biomechanical properties of the skin. Indeed, it has therefore been clearly described that during aging, there is a decrease in collagen synthesis, thinning of the dermis, a reduction in skin elasticity and suppleness and also

matrix disorganization.<sup>17,18</sup> As a result of all these effects, there is a marked age-related decline in the biomechanical properties of the skin.

Preliminary transcriptomic screening allowed us to identify the potential bioactivity of 4% mannose-6-phosphate complex after 6 hours of incubation on normal dermal fibroblasts. Among the gene significantly modified, we evidenced a very marked effect on dermal restructuring and remodeling. Indeed, mannose-6-phosphate complex significantly increased CTGF, CYR61, and TGFβ1 expression versus the untreated condition. CTGF codes for connective tissue growth factor which is a regulator of collagen

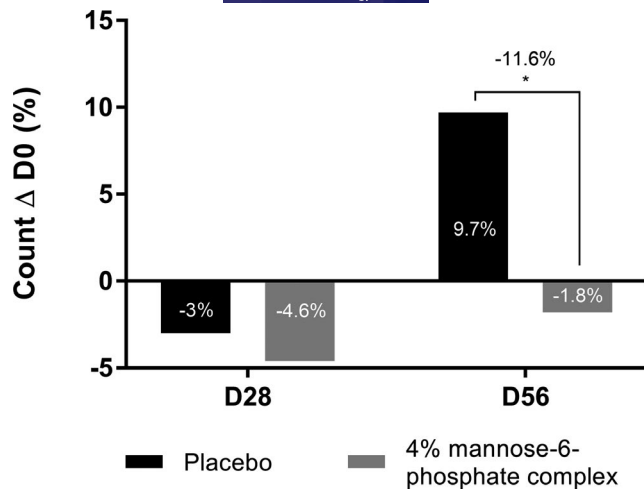


**FIGURE 9** Quantification of Crow's feet wrinkles with VISIA CR 2.3<sup>®</sup> analyzing system after 28 and 56 days of twice daily application in hemiface of a cream containing 4% mannose-6-phosphate complex versus placebo. Comparisons were made using Student's t test with \* $P < .05$

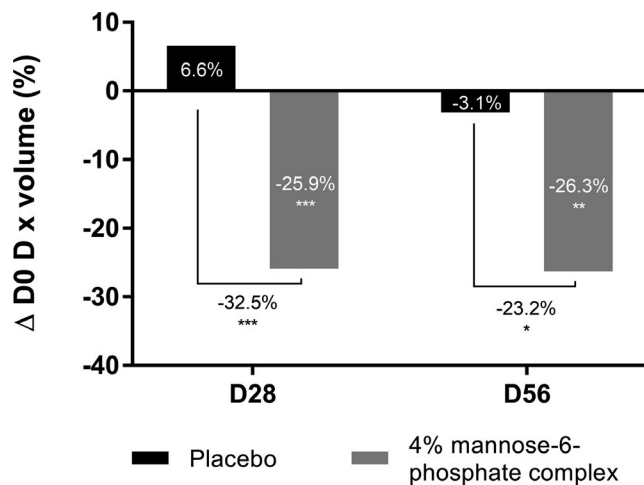


**FIGURE 10** Quantification of neck wrinkle volume with AEVA-HE<sup>®</sup> analyzing system after 28 and 56 days of twice daily application of a cream containing 4% mannose-6-phosphate complex vs placebo. Comparisons were made using Student's t test with \* $P < .05$ , \*\* $P < .01$ , \*\*\* $P < .001$

synthesis and its upregulation confirmed improvement of the extracellular matrix structure.<sup>28,30</sup> CYR61 codes for an extracellular matrix component which assists and stimulates skin fibroblast migration, encouraging regeneration and restructuring of the dermis.<sup>31</sup> The upregulation of TGF $\beta$ 1 RNA expression evidenced that dermis restructuring also occurs as a result of increased fibroblast proliferation.<sup>32</sup>

Through bibliographic research, we are aware that CTGF, CYR61, and TGF $\beta$  regulate structural proteins such as Collagen V, Fibulin-1, and Tenascin C. Moreover, these three proteins play a key role in dermal organization and cohesion. Collagen V is a fibrillar collagen and a minor component in the dermal matrix associated with collagen I fibres.<sup>7</sup> In the skin, Fibulin-1 is a component of the extracellular matrix

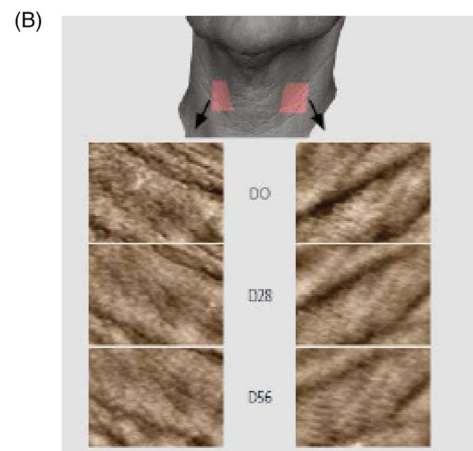
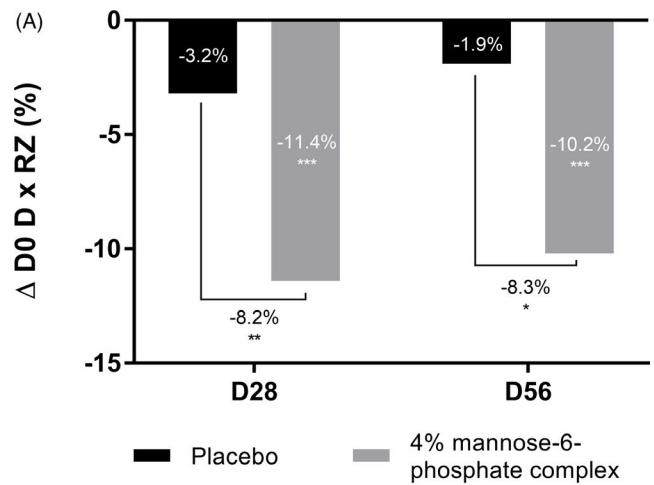


**FIGURE 11** Quantification of neck wrinkle depth using AEVA-HE<sup>®</sup> analyzing system (A) and 3D reconstruction of the neck (B) after 28 and 56 d of twice daily application of a cream containing 4% mannose-6-phosphate complex versus placebo. Comparisons were made using Student's t test with \* $P < .05$ , \*\* $P < .01$ , \*\*\* $P < .001$

but is also involved at the dermo-epidermal junction but with a very low level of expression.<sup>11</sup> Tenascin C is a matrix protein involved in cell cohesion at the dermo-epidermal junction and is located in the basal layers.<sup>12</sup> An ex vivo study of expression of these proteins by immunohistochemistry revealed that mannose-6-phosphate complex significantly increased their expression. These results strongly evidenced that mannose-6-phosphate complex significantly improved organization of the dermis through up-expression of key proteins involved in the structure and organization of the dermis. This was confirmed by morphological analysis by Masson's Trichrome staining which evidenced increased density in the reticular dermis with 4% mannose-6-phosphate complex treatment versus the untreated condition.

We identified AFM as an innovative method as a further advancement in our investigation of the potential improving effect of mannose-6-phosphate complex on skin restructuring and more specifically, on the biomechanical properties of the skin. Through the topographic mode of AFM, we were able to evidence the impact

of aging on the organization of collagen fibers in the reticular dermis. This loss of disorganization has been quantitatively confirmed by SAXS measurement, which is a complementary method to AFM. Consequently, we asked ourselves whether this disorganization of the collagen network could have an impact on Young's modulus in reticular dermis. Indeed, we evidenced a significant difference in the Young's modulus of dermis between young skin and mature skin, proving there is loss of skin firmness during aging. Following this proof of concept evidenced by the use of AFM, we sought to assess the impact of mannose-6-phosphate complex on these biomechanical properties. We evidenced that 4% mannose-6-phosphate complex had a major effect on improving the mechanical properties of mature skin, since it reorganized the collagen fiber network, leading to an increase in Young's modulus in reticular dermis in response to treatment, indicating an enhancing of skin firmness.

After observing the effect of mannose-6-phosphate complex on improving the collagen fiber network *ex vivo*, we asked ourselves how this could improve the biomechanical properties of the skin on a clinical level. Using SIAscope<sup>®</sup> measurement, we were able to quantify the collagen density in the skin by means of the light reemitted through interaction with collagen. By means of this method, we evidenced an increase in collagen density in the skin after 28 and 56 days of twice daily application to half the face of cream containing 4% mannose-6-phosphate complex versus placebo. There was indeed a marked effect after 28 days and 56 days of application with a 3.8-fold and 2.2-fold improvement in organization of the collagen network, respectively. As mannose-6-phosphate complex showed an improving effect in terms of skin collagen density, we wondered whether this increase in collagen might be related to a beneficial effect on wrinkles. To this end, we analyzed wrinkles focusing on those from the crow's feet area and observed that 4% mannose-6-phosphate complex improved the appearance of wrinkles by significantly reducing their number versus placebo after 56 days of application.

We subsequently wished to conduct further research to determine the impact of this active on a specific wrinkle formed as a result of mechanical stress, that is, neck wrinkles. Indeed, neck wrinkle formation is partly due to aging and sagging of the skin, but changes in head posture are also an important factor involved in this phenomenon since they increase mechanical stresses in this area.<sup>33</sup> As mannose-6-phosphate complex proved on an *ex vivo* level to have a beneficial impact on the biomechanical properties of the skin, we decided to evaluate its impact on neck wrinkle size and depth. As we hoped, mannose-6-phosphate complex significantly decreased neck wrinkle size and depth after 28 and 56 days in relation to day 0 and versus placebo on each occasion. We thus proved the efficiency of mannose-6-phosphate complex in improving the biomechanical properties of the skin, even in areas subject to biomechanical stress.

## 5 | CONCLUSION

In this study, we identified mannose-6-phosphate complex as a new powerful molecule capable of reversing the visible signs of

aging. Transcriptomic and immunohistochemistry studies identified an interesting biological effect in terms of dermal restructuring. By using AFM coupled to SAXS, we were able to highlight the effect of mannose-6-phosphate complex in improving the biomechanical properties of the skin, which are highly impacted during aging as evidenced in this study. AFM appeared to be a powerful and predictive method *ex vivo* use, since the results obtained were perfectly correlated with a marked improving effect, as confirmed by clinical studies using SIAscope<sup>®</sup>, VISIA CR 2.3<sup>®</sup> and AEVA-HE<sup>®</sup>. Mannose-6-phosphate was able to protect proteins of the dermis scaffold against oxidation and degradation, thereby allowing reorganization and a marked improvement in the biomechanical properties of the skin. The data that support the findings of this study are available from the corresponding author upon reasonable request.

## ACKNOWLEDGMENTS

We would like to thank P. Auriol, C. Paulus, B. Elbaum, E. Don Simoni, and D. Auriol for their contribution in the design and development of the mannose-6-phosphate complex. We thank J. Sandré and his team for their collaboration with Givaudan, allowing us working on fresh skin tissue and cells. We thank M. Meunier and A. Scandolera for their expertise in the management of *in vitro* and *ex vivo* studies. We also thank E. Chapuis and L. Lapierre for their expertise in the acquisition and analysis of clinical data. A. Scandolera and R. Reynaud are gratefully acknowledged for continuous support on this project and scientific discussions. The authors would like to Syntivia (Toulouse, France), (BIO-EC (Longjumeau, France), Novitom (Grenoble, France), and Biomeca (Lyon, France) for their great help in the completion of this paper.

## DATA AVAILABILITY STATEMENT

The data that support the findings of this study are available from the corresponding author upon reasonable request.

## ORCID

Marie Meunier  <https://orcid.org/0000-0003-2925-9094>

## REFERENCES

1. Wong R, Geyer S, Weninger W, Guimberteau J-C, Wong JK. The dynamic anatomy and patterning of skin. *Exp Dermatol*. 2016;25(2):92-98.
2. Pullar J, Carr A, Vissers M. The roles of vitamin C in skin health. *Nutrients*. 2017;9(8):866.
3. Meigel WN, Gay S, Weber L. Dermal architecture and collagen type distribution. *Archi Dermatol Res*. 1977;259(1):1-10.
4. Guilbert M, Roig B, Terryn C, et al. Highlighting the impact of aging on type I collagen: label-free investigation using confocal reflectance microscopy and diffuse reflectance spectroscopy in 3D matrix model. *Oncotarget*. 2016;7(8):8546-8555.
5. Alves R, Ferreira L, Vale E, Bordalo O. Pseudoxanthoma elasticum papillary dermal elastolysis: a case report. *Dermatol Res Pract*. 2010;2010:1-4.
6. Fenner J, Clark RAF. Anatomy, Physiology, Histology, and Immunohistochemistry of Human Skin. *Skin Tissue Engineering and Regenerative Medicine*. Academic Press; 2016:1-17.

7. Wenstrup RJ, Florer JB, Brunskill EW, Bell SM, Chervoneva I, Birk DE. Type V collagen controls the initiation of collagen fibril assembly. *J Biol Chem*. 2004;279(51):53331-53337.
8. Muiznieks LD, Keeley FW. Molecular assembly and mechanical properties of the extracellular matrix: A fibrous protein perspective. *Biochim Biophys Acta-Mol Basis Dis*. 2013;1832(7):866-875.
9. Dyer JM, Miller RA. Chronic skin fragility of aging: current concepts in the pathogenesis. *Recogn Manag Dermatoporosis*. 2018;11(1):6.
10. Langton AK, Graham HK, McConnell JC, Sherratt MJ, Griffiths CEM, Watson REB. Organization of the dermal matrix impacts the biomechanical properties of skin. *Br J Dermatol*. 2017;177(3):818-827.
11. Roark EF, Keene DR, Haudenschild CC, Godyna S, Little CD, Argraves WS. The association of human fibulin-1 with elastic fibers: an immunohistological, ultrastructural, and RNA study. *J Histochem Cytochem*. 1995;43(4):401-411.
12. Filsell R, Jenkins G. Coordinate upregulation of tenascin C expression with degree of photodamage in human skin. *Br J Dermatol*. 1999;140(4):592-599.
13. Basisty N, Holtz A, Schilling B. Accumulation of "Old Proteins" and the critical need for ms-based protein turnover measurements in aging and longevity. *Proteomics*. 2020;20(5-6):1800403.
14. Li Y, Lei D, Swindell WR, et al. Age-Associated Increase in Skin Fibroblast-Derived Prostaglandin E 2 Contributes to Reduced Collagen Levels in Elderly Human Skin. *J Invest Dermatol*. 2015;135(9):2181-2188.
15. Varani J, Dame MK, Rittie L, et al. Decreased collagen production in chronologically aged skin. *Am J Pathol*. 2006;168(6):1861-1868.
16. Shin J-W, Kwon S-H, Choi J-Y, et al. Molecular mechanisms of dermal aging and antiaging approaches. *Int J Mol Sci*. 2019;20(9):2126.
17. Ganceviciene R, Liakou AI, Theodoridis A, Makrantonaki E, Zouboulis CC. Skin anti-aging strategies. *Dermato-Endocrinology*. 2012;4(3):308-319.
18. Kular JK, Basu S, Sharma RI. The extracellular matrix: Structure, composition, age-related differences, tools for analysis and applications for tissue engineering. *J Tissue Eng*. 2014;5:204173141455711.
19. Diridollou S, Vabre V, Berson M, et al. Skin ageing: changes of physical properties of human skin *in vivo*: Skin ageing. *Int J Cosmet Sci*. 2001;23(6):353-362.
20. Kaur A, Ecker BL, Douglass SM, et al. Remodeling of the collagen matrix in aging skin promotes melanoma metastasis and affects immune cell motility. *Cancer Discov*. 2019;9(1):64-81.
21. Silver FH, Sehra GP, Freeman JW, DeVore D. Viscoelastic properties of young and old human dermis: A proposed molecular mechanism for elastic energy storage in collagen and elastin. *J Appl Polymer Sci*. 2002;86(8):1978-1985.
22. Zahouani H, Boyer G, Paillet-Mattei C, Ben Tkaya M, Vargiolu R. Effect of human ageing on skin rheology and tribology. *Wear*. 2011;271(9-10):2364-2369.
23. Binnig GK. Atomic force microscope and method for imaging surfaces with atomic resolution. Published online February 9, 1988.
24. Cappella B, Dietler G. Force-distance curves by atomic force microscopy. *Surf Sci Rep*. 1999;34(1-3):1-104.
25. Geisse NA. AFM and combined optical techniques. *Mater Today*. 2009;12(7-8):40-45.
26. Alsteens D, Dupres V, Yunus S, Latgé J-P, Heinisch JJ, Dufrêne YF. High-resolution imaging of chemical and biological sites on living cells using peak force tapping atomic force microscopy. *Langmuir*. 2012;28(49):16738-16744.
27. Moger CJ, Barrett R, Bleuet P, et al. Regional variations of collagen orientation in normal and diseased articular cartilage and subchondral bone determined using small angle X-ray scattering (SAXS). *Osteoarthritis Cartilage*. 2007;15(6):682-687.
28. Sharma V, Ichikawa M, Freeze HH. Mannose metabolism: More than meets the eye. *Biochem Biophys Res Commun*. 2014;453(2):220-228.
29. Göran RK. Extracellular vesicles and energy metabolism. *Clin Chim Acta*. 2019;488:116-121.
30. Quan T, Shao Y, He T, Voorhees JJ, Fisher GJ. Reduced expression of connective tissue growth factor (CTGF/CCN2) mediates collagen loss in chronologically aged human skin. *J Invest Dermatol*. 2010;130(2):415-424.
31. Chen N, Chen C-C, Lau LF. Adhesion of Human Skin Fibroblasts to Cyr61 Is Mediated through Integrin  $\alpha_6\beta_1$  and Cell Surface Heparan Sulfate Proteoglycans. *J Biol Chem*. 2000;275(32):24953-24961.
32. Liu Y, Li Y, Li N, et al. TGF- $\beta$ 1 promotes scar fibroblasts proliferation and transdifferentiation via up-regulating MicroRNA-21. *Sci Rep*. 2016;6(1):1-9.
33. Hyun MY, Li K, Kim BJ, et al. Novel treatment of neck wrinkles with an intradermal radiofrequency device. *Ann Dermatol*. 2015;27(1):79.

**How to cite this article:** Meunier M, Chapuis E, Lapierre L, et al. Mannose-6-phosphate complex and improvement in biomechanical properties of the skin. *J Cosmet Dermatol*. 2021;20:1598-1610. <https://doi.org/10.1111/jocd.14000>